Paradoxes for chromonic liquid crystal droplets

Silvia Paparini [*] and Epifanio G. Virga [†]
Dipartimento di Matematica, Università di Pavia, Via Ferrata 5, 27100 Pavia, Italy

(Received 7 July 2022; accepted 2 October 2022; published 17 October 2022)

Chromonic liquid crystals constitute a novel lyotropic phase, whose elastic properties have so far been modeled within the classical Oseen-Frank theory, provided that the twist constant is assumed to be considerably smaller than the saddle-splay constant, in violation of one Ericksen inequality. This paper shows that paradoxical consequences follow from such a violation for droplets of these materials surrounded by an isotropic fluid. For example, tactoids with a degenerate planar anchoring simply disintegrate indefinitely in myriads of smaller ones.

DOI: 10.1103/PhysRevE.106.044703

I. INTRODUCTION

Chromonic liquid crystals (CLCs) are lyotropic materials, which include Sunset Yellow (SSY), a popular dye in food industry, and disodium cromoglycate (DSCG), an antiasthmatic drug. In these materials, molecules stuck themselves in columns, which in aqueous solutions develop a nematic orientational order, described by a unit vector field $\boldsymbol{n}$, called the *director*, representing the average direction in space of the constituting supra-molecular aggregates. A number of reviews have already appeared in the literature [1–5], to which we refer the reader.

Experiments have been performed with these materials in capillary tubes, with either circular [6,7] or rectangular [8] cross-sections, as well as on cylindrical shells [9], all enforcing *degenerate planar* anchoring, which allows constituting columns to glide freely on the anchoring surface, provided they remain tangent to it. These experiments revealed a tendency of CLCs to acquire in cylinders a *twisted* configuration at equilibrium, which is represented by an *escaped twist* (ET) director field.

Despite the lack of uniformity in the ground state of these phases [10], they have been modeled by the classical Oseen-Frank theory of nematic liquid crystals, albeit with an anomalously small twist constant K_{22}. To accommodate the experimental findings and justify the twisted ground state, this constant has to be smaller than the saddle-splay constant K_{24}, in violation of one of the inequalities Ericksen [11] had put forward to guarantee that the Oseen-Frank free-energy density be bounded below.

Actually, as shown in Ref. [12], such a violation does not prevent the twisted ground state from being locally stable in a cylinder enforcing degenerate planar anchoring. The same reassuring conclusion was reached in Ref. [13]. But the question remained as to whether different boundary conditions, still physically significant, could unleash the unboundedness of the total free energy potentially related to the violation of one Ericksen inequality (see also Ref. [13] in this connection).

In this paper, we answer this question for the *positive*. If $K_{22} < K_{24}$, a CLC droplet, tactoidal[1] in shape and surrounded by an isotropic fluid environment enforcing degenerate planar anchoring for the director, is predicted to be unstable against *shape change*: it would split indefinitely in smaller tactoids while the total free energy plummets to negative infinity.

This prediction is in sharp contrast with the wealth of experimental observations of CLC tactoidal droplets, stable in the biphasic region of phase space, where nematic and isotropic phases coexist in equilibrium. Experiments have been carried out with a number of substances (including DSCG and SSY) stabilized by the addition of neutral (achiral) condensing agents (such as PEG and Spm) [14–18]. These studies have consistently reported stable twisted bipolar tactoids. Here is our conundrum: if we adopt the Oseen-Frank theory to describe CLCs, then we need to assume that $K_{24} > K_{22}$ to explain the twisted nematic textures observed in cylindrical capillaries, but we also need to assume that $K_{24} < K_{22}$ to justify the very existence of the twisted tactoids observed in the biphasic coexistence region.

A similar paradoxical behavior is expected if the splay constant K_{11} is anomalously small. If $K_{11} < K_{24}$, in violation of another Ericksen inequality, a spherical CLC droplet surrounded by a fluid environment enforcing *homeotropic*[2] anchoring would split indefinitely in smaller spherical droplets, while the total free energy diverges to negative infinity.

The paper is organized as follows. In Sec. II we recall a *modicum* of the classical Oseen-Frank theory for nematic liquid crystals, including all Ericksen inequalities. In Sec. III, we set the scene for the free-boundary problem that need be solved to identify the sequences of shapes that fragment a parent drop proving it unstable. Sections IV and V are devoted to the explicit construction of such sequences for cases in which one or the other of two Ericksen inequalities are violated. In

[*] silvia.paparini@unipv.it
[†] eg.virga@unipv.it

[1] *Tactoids* are elongated, cylindrically symmetric shapes with pointed ends as poles.

[2] That is, with $\boldsymbol{n}$ along the outer unit normal.

Sec. VI, we draw the conclusions of this work, casting doubts on the applicability of the Oseen-Frank theory to describe the elasticity of CLCs. This is our attitude to account for the body of experimental evidence observed in both capillary tubes and twisted tactoids, as within the Oseen-Frank framework the former would justify violating some Ericksen inequalities, whereas the latter would require them to be valid. The paper is closed by five Appendices, where a number of mathematical proofs are relegated to ease reading the main text.

II. CLASSICAL ELASTIC THEORY

The classical elastic theory of liquid crystals goes back to the pioneering works of Oseen [19] and Frank [20].[3] This theory is variational in nature, as it is based on a bulk free-energy functional $\mathscr{F}_{\rm b}$ written in the form

$$\mathscr{F}_{\rm b}[\boldsymbol{n}] := \int_{\mathscr{B}} W_{\rm OF}(\boldsymbol{n}, \nabla\boldsymbol{n})dV, \tag{1}$$

where $\mathscr{B}$ is a region in space occupied by the material and V is the volume measure. In Eq. (1), $W_{\rm OF}$ measures the distortional cost produced by a deviation from a uniform director field $\boldsymbol{n}$. It is chosen to be the most general frame-indifferent,[4] even function quadratic in $\nabla\boldsymbol{n}$,

$$\begin{aligned} W_{\rm OF}(\boldsymbol{n}, \nabla\boldsymbol{n}) := {} & \tfrac{1}{2}K_{11}(\operatorname{div}\boldsymbol{n})^2 + \tfrac{1}{2}K_{22}(\boldsymbol{n}\cdot\operatorname{curl}\boldsymbol{n})^2 \\ & + \tfrac{1}{2}K_{33}|\boldsymbol{n}\times\operatorname{curl}\boldsymbol{n}|^2 \\ & + K_{24}[\operatorname{tr}(\nabla\boldsymbol{n})^2 - (\operatorname{div}\boldsymbol{n})^2]. \end{aligned} \tag{2}$$

Here K_{11}, K_{22}, K_{33}, and K_{24} are elastic constants characteristic of the material. They are often referred to as the *splay*, *twist*, *bend*, and *saddle-splay* constants, respectively, by the features of the different orientation fields, each with a distortion energy proportional to a single term in Eq. (2) (see, for example, Ch. 3 of Ref. [22]).

Recently, Selinger [23] has reinterpreted the classical formula (2) by decomposing the saddle-splay mode into a set of other independent modes. The starting point of this decomposition is a novel representation of $\nabla\boldsymbol{n}$ (see also Ref. [24]),

$$\nabla\boldsymbol{n} = -\boldsymbol{b}\otimes\boldsymbol{n} + \tfrac{1}{2}T\mathbf{W}(\boldsymbol{n}) + \tfrac{1}{2}S\mathbf{P}(\boldsymbol{n}) + \mathbf{D}, \tag{3}$$

where $\boldsymbol{b} := -(\nabla\boldsymbol{n})\boldsymbol{n} = \boldsymbol{n}\times\operatorname{curl}\boldsymbol{n}$ is the *bend* vector, $T := \boldsymbol{n}\cdot\operatorname{curl}\boldsymbol{n}$ is the *twist*, $S := \operatorname{div}\boldsymbol{n}$ is the *splay*, $\mathbf{W}(\boldsymbol{n})$ is the skew-symmetric tensor that has $\boldsymbol{n}$ as axial vector, $\mathbf{P}(\boldsymbol{n}) := \mathbf{I} - \boldsymbol{n}\otimes\boldsymbol{n}$ is the projection onto the plane orthogonal to $\boldsymbol{n}$, and $\mathbf{D}$ is a symmetric tensor such that $\mathbf{D}\boldsymbol{n} = \mathbf{0}$ and $\operatorname{tr}\mathbf{D} = 0$.

By its own definition, $\mathbf{D} \neq \mathbf{0}$ admits the following biaxial representation:

$$\mathbf{D} = q(\boldsymbol{n}_1\otimes\boldsymbol{n}_1 - \boldsymbol{n}_2\otimes\boldsymbol{n}_2), \tag{4}$$

where $q > 0$ and $(\boldsymbol{n}_1, \boldsymbol{n}_2)$ is a pair of orthogonal unit vectors in the plane orthogonal to $\boldsymbol{n}$, oriented so that $\boldsymbol{n} = \boldsymbol{n}_1\times\boldsymbol{n}_2$.[5]

By use of the following identity:

$$2q^2 = \operatorname{tr}(\nabla\boldsymbol{n})^2 + \tfrac{1}{2}T^2 - \tfrac{1}{2}S^2, \tag{5}$$

we can easily give Eq. (2) the equivalent form,

$$\begin{aligned} W_{\rm OF}(\boldsymbol{n}, \nabla\boldsymbol{n}) = {} & \tfrac{1}{2}(K_{11} - K_{24})S^2 + \tfrac{1}{2}(K_{22} - K_{24})T^2 \\ & + \tfrac{1}{2}K_{33}B^2 + 2K_{24}q^2, \end{aligned} \tag{6}$$

where $B^2 := \boldsymbol{b}\cdot\boldsymbol{b}$. Since (S, T, B, q) are all independent *distortion characteristics*, it readily follows from Eq. (6) that $W_{\rm OF}$ is positive semidefinite whenever

$$K_{11} \geqq K_{24} \geqq 0, \tag{7a}$$

$$K_{22} \geqq K_{24} \geqq 0, \tag{7b}$$

$$K_{33} \geqq 0, \tag{7c}$$

which are the celebrated *Ericksen's inequalities* [11]. If these inequalities are satisfied in strict form, the global ground state of $W_{\rm OF}$ is attained on the uniform director field, characterized by

$$S = T = B = q = 0. \tag{8}$$

As already mentioned in the Introduction, inequality (7b) must be violated for the ground state of $W_{\rm OF}$ to be different from Eq. (8), involving a nonvanishing T. We shall see below how such a choice entails paradoxical consequences.

Liquid crystals are (within good approximation) incompressible fluids. Thus, when the region $\mathscr{B}$ is *not* fixed, as in the cases considered in this paper, for a given amount of material, $\mathscr{B}$ is subject to the *isoperimetric* constraint that prescribes its volume,

$$V(\mathscr{B}) = V_0. \tag{9}$$

When $\mathscr{B}$ is surrounded by an isotropic fluid, a surface energy arises at the free interface $\partial\mathscr{B}$, which, following Ref. [27], we represent as

$$\mathscr{F}_{\rm s}[\boldsymbol{n}] := \int_{\partial\mathscr{B}} \gamma[1 + \omega(\boldsymbol{n}\cdot\boldsymbol{\nu})^2]dA, \tag{10}$$

where $\boldsymbol{\nu}$ is the outer unit normal to $\partial\mathscr{B}$, $\gamma > 0$ is the *isotropic* surface tension, and $\omega > -1$ is a dimensionless parameter weighting the *anisotropic* component of surface tension. For $\omega > 0$, $\mathscr{F}_{\rm s}$ promotes the *degenerate planar* anchoring, whereas for $\omega < 0$, it promotes the *homeotropic* anchoring. The total free-energy functional will then be written as

$$\mathscr{F}[\boldsymbol{n}] := \mathscr{F}_{\rm b}[\boldsymbol{n}] + \mathscr{F}_{\rm s}[\boldsymbol{n}]. \tag{11}$$

[3] Also a paper by Zocher [21], mainly concerned with the effect of a magnetic field on director distortions, is often mentioned among the founding contributions. Some go to the extent of also naming the theory after him. Others, in contrast, name the theory only after Frank, as they only deem his contribution to be fully aware of the nature of $\boldsymbol{n}$ as a *mesoscopic* descriptor of molecular order.

[4] A function $W(\boldsymbol{n}, \nabla\boldsymbol{n})$ is *frame-indifferent* if it is invariant under the action of the orthogonal group $\mathsf{O}(3)$, that is, if $W(\mathbf{Q}\boldsymbol{n}, \mathbf{Q}(\nabla\boldsymbol{n})\mathbf{Q}^{\mathsf{T}}) = W(\boldsymbol{n}, \nabla\boldsymbol{n})$ for all $\mathbf{Q} \in \mathsf{O}(3)$, where $\mathbf{Q}^{\mathsf{T}}$ denotes the transpose of $\mathbf{Q}$.

[5] It is argued in Ref. [25] that q should be given the name *tetrahedral* splay, to which we would actually prefer *octupolar* splay for the role played by a cubic (octupolar) potential on the unit sphere [26] in representing all scalar measures of distortion, but T.

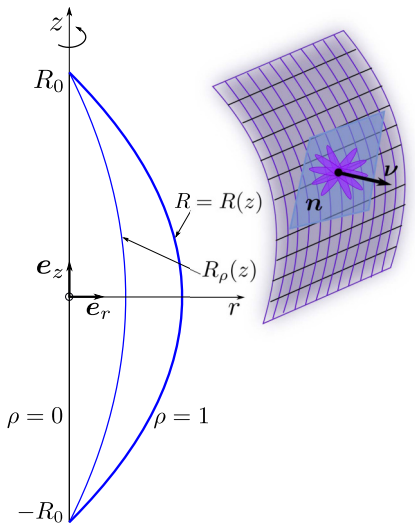

FIG. 1. The function $R(z)$ represents the boundary $\partial\mathscr{B}$, while $R_\rho(z) = \rho R(z)$, for $\rho \in [0, 1]$, is the retraction of $R(z)$, representing a surface on which the polar angle β is constant. The director field is tangent to the boundary, but free to orient itself in any direction, as illustrated by the sketch on the side.

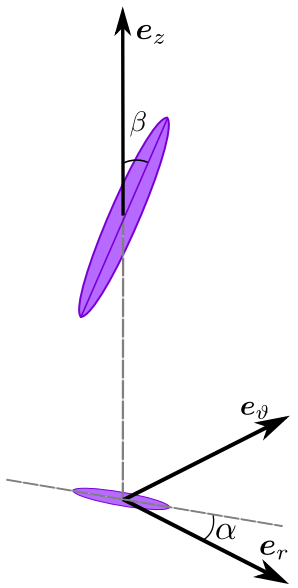

FIG. 2. The director field $\boldsymbol{n}$ is described by the azimuthal angle α, which the projection of $\boldsymbol{n}$ on the (r, ϑ) plane makes with $\boldsymbol{e}_r$, and the polar angle β, which $\boldsymbol{n}$ makes with the drop's symmetry axis $\boldsymbol{e}_z$.

III. FREE-BOUNDARY PROBLEM

A drop comprising a given quantity of CLC is free to adjust its shape $\mathscr{B}$ when surrounded by an isotropic environment, subject only to Eq. (9). In particular, we assume that $\mathscr{B}$ is a region in three-dimensional space rotationally symmetric about the z-axis of a standard cylindrical frame $(\boldsymbol{e}_r, \boldsymbol{e}_\vartheta, \boldsymbol{e}_z)$. As shown in Fig. 1, the boundary $\partial\mathscr{B}$ is obtained by rotating the graph of a smooth function, $R = R(z)$, which represents the radius of the drop's cross-section at height $z \in [-R_0, R_0]$. The function R vanishes at $z = \pm R_0$, where the drop has its *poles*. As in Ref. [28] [see, for example, Eqs. (19) and (20)], the volume of $\mathscr{B}$ can be expressed in terms of the function $R(z)$ as

$$V(\mathscr{B}) = \pi \int_{-R_0}^{R_0} R^2(z)dz, \tag{12}$$

and the area of $\partial\mathscr{B}$ as

$$A(\partial\mathscr{B}) = \pi \int_{-R_0}^{R_0} R(z)\sqrt{1 + R'(z)^2}dz. \tag{13}$$

Here and below, a prime $'$ will denote differentiation.

The only requirement for the director $\boldsymbol{n}$ at the free surface of the drop is to fulfill the *degenerate planar* condition,

$$\boldsymbol{n}|_{\partial\mathscr{B}} \cdot \boldsymbol{\nu} = 0, \tag{14}$$

which here, for simplicity, is imposed as a constraint. As a consequence of Eq. (14), the surface free energy $\mathscr{F}_s$ reduces to

$$\mathscr{F}_s[\boldsymbol{n}] = \gamma A(\partial\mathscr{B}). \tag{15}$$

In the present setting, $A(\partial\mathscr{B})$ is given by Eq. (13) and $\boldsymbol{\nu}$ is written as

$$\boldsymbol{\nu} = \frac{\boldsymbol{e}_r - R'\boldsymbol{e}_z}{\sqrt{1 + R'^2}}. \tag{16}$$

For $\boldsymbol{n}$ to be tangent to $\partial\mathscr{B}$, it should be allowed to flip out the plane $(\boldsymbol{e}_\vartheta, \boldsymbol{e}_z)$. The class of admissible director fields will thus be described by

$$\boldsymbol{n} = \cos\alpha \sin\beta \boldsymbol{e}_r + \sin\alpha \sin\beta \boldsymbol{e}_\vartheta + \cos\beta \boldsymbol{e}_z, \tag{17}$$

where $\alpha \in [0, 2\pi)$ is the *azimuthal* angle and $\beta \in [0, \pi]$ is the *polar* angle (see Fig. 2). Here, we shall assume that α depends only on z, $\alpha = \alpha(z)$, while β depends on both r and z, but only through the ratio

$$\rho := \frac{r}{R(z)} \in [0, 1]. \tag{18}$$

The rationale behind this choice is to let β be constant on $\partial\mathscr{B}$, where $r = R(z)$ and $\rho = 1$, and on all surfaces in the interior of $\mathscr{B}$ obtained from $\partial\mathscr{B}$ by a *linear retraction* towards the symmetry axis z, represented by $R_\rho(z) := \rho R(z)$ with $0 \leqq \rho < 1$ (see Fig. 1). By letting $\beta = \beta(\rho)$, we assign a polar angle to each retracted surface, the value on one surface being possibly different from the value on other surfaces. Since all retracted surfaces fill the drop, the director field $\boldsymbol{n}$ is defined on the whole of $\mathscr{B}$ through only two scalar-valued functions in a single variable, $\alpha(z)$ and $\beta(\rho)$. The constraint in Eq. (14) makes these functions not independent, as with the aid of Eq. (16) we see from Eq. (17) that Eq. (14) is valid only if

$$\cos\alpha(z) = \frac{R'(z)}{\tan\beta(1)}, \tag{19}$$

which amounts to the alternative,

$$\alpha(z) = \begin{cases} \arccos\left[\frac{R'(z)}{\tan\beta(1)}\right], \\ 2\pi - \arccos\left[\frac{R'(z)}{\tan\beta(1)}\right], \end{cases} \tag{20}$$

whose meaning will soon become clear. Meanwhile, we note that a new constraint arises from Eq. (19) for R', that is,

$$-|\tan\beta(1)| \leqq R'(z) \leqq |\tan\beta(1)|. \tag{21}$$

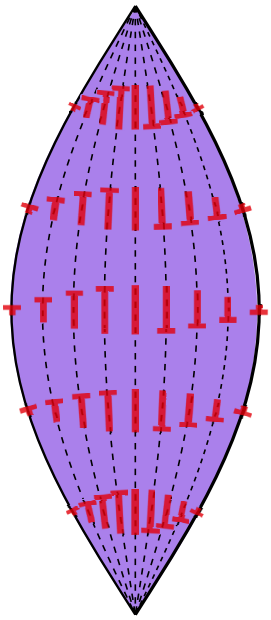

FIG. 3. A tactoid with a twisted nematic director field represented as in Eqs. (17) and (20). The (r, z) plane of the drawing is a symmetry plane of the drop through its axis. A (red) segment represents $\boldsymbol{n}$ when it lies on the plane of the drawing, while a nail is used for the projection of $\boldsymbol{n}$ on that plane when the director is askew with it, the head designating conventionally the end on the same side as the viewer. Dashed lines are cross-sections of the surfaces representing retractions of the boundary.

Figure 3 illustrates our construction for a *twisted tactoid*: it shows a meridian cross-section of the drop with its family of retracted surfaces to which $\boldsymbol{n}$ is everywhere tangent. Generically, the director does not lie on the plane of the drawing (spanned by $\boldsymbol{e}_r$ and $\boldsymbol{e}_z$), as indicated by the nail symbols, whose heads are conventionally above that plane. Neither is the projection of $\boldsymbol{n}$ on the (r, z) plane tangent everywhere to the lines representing the retracted boundary for $0 < \rho < 1$. This is confirmed by a careful inspection of Fig. 3, but is perhaps better revealed by noting that the outer unit normal $\boldsymbol{\nu}_\rho$ to the retracted surface represented by R_ρ is

$$\boldsymbol{\nu}_\rho = \frac{\boldsymbol{e}_r - R'_\rho(z)\boldsymbol{e}_z}{\sqrt{1 + R'^2_\rho}} \tag{22}$$

and that, consequently,

$$\boldsymbol{n} \cdot \boldsymbol{\nu}_\rho = \frac{R'(z)\cos\beta(\rho)}{\sqrt{1 + R'^2_\rho(z)}}\left[\frac{\tan\beta(\rho)}{\tan\beta(1)} - \rho\right]. \tag{23}$$

In particular, the latter formula shows that the nails depicted in Fig. 3 are tangent to the cross-sections of the surfaces retracting the boundary on the symmetry plane $z = 0$ and, of course, for $\rho = 1$ and $\rho = 0$ [if, by symmetry, we assume that $\tan\beta(0) = 0$]. Finally, choosing one instead of the other alternative in Eq. (20) amounts to swap head and tails in the nails.

Standard computations (deferred to Appendix A) show that the distortion characteristics associated with the field in Eq. (17) are given by

$$S = \frac{1}{R}\left(\cos\alpha\cos\beta\beta' + \frac{1}{\rho}\cos\alpha\sin\beta + \rho R'\sin\beta\beta'\right), \tag{24a}$$

$$T = \frac{1}{R}\left[\sin\alpha\left(\beta' + \frac{1}{\rho}\cos\beta\sin\beta\right) - \sin^2\beta\alpha' R\right], \tag{24b}$$

$$B^2 = \frac{1}{R^2}\left[\beta'^2(\rho R'\cos\beta - \cos\alpha\sin\beta)^2 + \sin^2\beta\left(\alpha' R\cos\beta + \frac{1}{\rho}\sin\alpha\sin\beta\right)\right], \tag{24c}$$

$$\begin{aligned} 2q^2 = \frac{1}{R^2}\Bigg\{&\frac{\beta'^2}{2}[(\cos\alpha\cos\beta + \rho R'\sin\beta)^2 + \sin^2\alpha] + \frac{1}{2\rho^2}\sin^2\beta(1 - \sin^2\alpha\sin^2\beta) \\ &- \frac{1}{\rho}\cos\beta\sin\beta\beta' + \frac{1}{2}(\alpha' R)^2\sin^4\beta + \sin\alpha\sin^2\beta(\alpha' R)(\beta' - \cos\beta\sin\beta) - R'\cos\alpha\sin^2\beta\beta'\Bigg\}. \end{aligned} \tag{24d}$$

In particular, Eq. (24b) shows that, for given β, changing the representation of α in accordance with Eq. (20) only changes the sign of T, thus indicating that the two alternative representations of α in Eq. (20) correspond to two director fields with opposite *helicity*, that is, winding in opposite senses around the drop's axis. Since both representations for α in Eq. (20) are equivalent, hereafter, for definiteness, we shall choose the first, with no prejudice for the generality of our development.

We denote by R_e the *equivalent* radius, that is, the radius of a spherical drop with volume V_0, and by 2μ the span (at the poles) of the drop, scaled to the equivalent diameter $2R_e$,

$$\mu := \frac{R_0}{R_e} > 0. \tag{25}$$

We also rescale lengths r, z and $R(z)$ to R_e, leaving their names unaltered; with such a renormalization, we further set

$$U(\xi) := \sqrt{\mu} R[z(\xi)], \tag{26}$$

where ξ is defined by

$$\xi := \frac{z}{\mu} \in [-1, 1]. \tag{27}$$

With the aid of Eq. (12), the volume constraint (9) then simply reads as

$$\int_{-1}^{1} U(\xi)^2 d\xi = \frac{4}{3}. \tag{28}$$

For clarity and later use, we record here the form that Eq. (26) acquires in the original dimensional quantities,

$$U\left(\frac{z}{\mu R_{\rm e}}\right)=\frac{\sqrt{\mu}}{R_{\rm e}}R(z). \tag{29}$$

Furthermore, the function U must vanish at the poles,

$$U(\pm 1)=0, \tag{30}$$

and, by Eq. (21), its derivative is subject to the restriction

$$-\mu^{3/2}|\tan\beta(1)|\leqq U'(\xi)\leqq\mu^{3/2}|\tan\beta(1)|. \tag{31}$$

For example, for an even, concave function (corresponding to a convex drop $\mathscr{B}$), it would suffice that constraint (31) be obeyed for a given $\mu=\mu_0$ and at $\xi=1$, for it to be valid for all $\mu>\mu_0$ and for all $\xi\in[-1,1]$. On the other hand, smooth shapes are not allowed by Eq. (31), as for them $\lim_{\xi\to\pm1}U'(\xi)=\mp\infty$. Thus, hereafter we shall only consider *tactoids*, like the one represented in Fig. 3, for which U' is everywhere bounded.

By use of Eqs. (19), (20), (24), and both changes of variables (18) and (27), we give the bulk and surface free energies the following forms:

$$\begin{aligned}\mathcal{F}_{\rm b}[U,\beta;\mu]&:=\frac{\mathscr{F}_{\rm b}[\boldsymbol{n}]}{2\pi K_{22}R_{\rm e}}\\&=\frac{1}{\mu^2}\left[\int_{-1}^{1}U'(\xi)^2d\xi\right]\mathcal{F}_1[\beta]\\&\quad+\frac{1}{\mu^2}\left[\int_{-1}^{1}\frac{U(\xi)^2U''(\xi)^2}{\mu^3\tan^2\beta(1)-U'(\xi)^2}d\xi\right]\mathcal{F}_2[\beta]\\&\quad+\mu\mathcal{F}_3[\beta]\end{aligned} \tag{32a}$$

and

$$\mathcal{F}_{\rm s}[U;\mu,\upsilon]:=\frac{\mathscr{F}_{\rm s}[\boldsymbol{n}]}{2\pi K_{22}R_{\rm e}}=\upsilon\sqrt{\mu}\int_{-1}^{1}U(\xi)\sqrt{1+\frac{U'(\xi)^2}{\mu}}d\xi, \tag{32b}$$

where

$$\upsilon:=\frac{\gamma R_{\rm e}}{K_{22}} \tag{33}$$

is a reduced (dimensionless) volume, and the following notation has been employed,

$$\begin{aligned}\mathcal{F}_1[\beta]:=\int_0^1\Bigg\{&\frac{1}{\tan^2\beta(1)}\left[\frac{\beta'^2}{2}(k_1\cos^2\beta+k_3\sin^2\beta-1)+\frac{1}{2\rho^2}(k_1\sin^2\beta-\cos^2\beta\sin^2\beta+k_3\sin^4\beta)+\frac{(k_1-1)}{\rho}\cos\beta\sin\beta\beta'\right]\\&+\frac{1}{\tan\beta(1)}\left[\rho\cos\beta\sin\beta\beta'^2(k_1-k_3)+\sin^2\beta\beta'(k_1-1)+\frac{1}{\rho}\cos\beta\sin^3\beta(k_3-1)\right]\\&+\left[\frac{\rho^2\beta'^2}{2}(k_1\sin^2\beta+k_3\cos^2\beta)\right]\Bigg\}\rho d\rho,\end{aligned} \tag{34a}$$

$$\mathcal{F}_2[\beta]:=\int_0^1\frac{\sin^2\beta}{2}(\sin^2\beta+k_3\cos^2\beta)\rho d\rho, \tag{34b}$$

$$\mathcal{F}_3[\beta]:=\int_0^1\left[\frac{\beta'^2}{2}+\frac{1}{2\rho^2}\cos^2\beta\sin^2\beta+\frac{k_3}{2\rho^2}\sin^4\beta\right]\rho d\rho+\frac{(1-2k_{24})}{2}\sin^2\beta(1), \tag{34c}$$

which feature the *scaled* elastic constants defined as

$$k_1:=\frac{K_{11}}{K_{22}},\quad k_3:=\frac{K_{33}}{K_{22}},\quad k_{24}:=\frac{K_{24}}{K_{22}}. \tag{35}$$

The functionals in Eq. (34) depend only on the polar angle $\beta=\beta(\rho)$. For both $\mathcal{F}_1$ and $\mathcal{F}_3$ to be finite, β must satisfy the condition

$$\sin\beta(0)=0, \tag{36}$$

which entails that $\boldsymbol{n}$ is parallel to $\boldsymbol{e}_z$ along the drop's axis. As shown in Appendix A, the dependence of $\mathcal{F}_{\rm b}$ on α is hidden in $U'(\xi)$ and $\tan\beta(1)$ through the relation (19) rewritten in the new coordinate ξ in Eq. (27) as

$$\cos\alpha[z(\xi)]=\frac{U'(\xi)}{\mu^{3/2}\tan\beta(1)}. \tag{37}$$

Finally, the appropriate dimensionless form of the total free energy $\mathscr{F}$ in Eq. (11) is expressed as the sum of the expressions in Eqs. (32a) and (32b):

$$\mathcal{F}[U,\beta;\mu,\upsilon]:=\frac{\mathscr{F}[\boldsymbol{n}]}{2\pi K_{22}R_{\rm e}}=\mathcal{F}_{\rm b}[U,\beta;\mu]+\mathcal{F}_{\rm s}[U;\mu,\upsilon], \tag{38}$$

where the role of parameters μ and υ is distinguished from that of functions U and β for later convenience. In the following sections, we shall make use of this expression for $\mathcal{F}$ to show that for either $K_{22}<K_{24}$ or $K_{11}<K_{24}$ there are sequences of droplets, which the drop $\mathscr{B}$ can disintegrate in, so that the total volume V_0 is preserved, but the total free energy plummets to $-\infty$. These sequences will provide ground for paradoxes.

IV. VIOLATING $K_{22}\geqq K_{24}$

Here, we construct a family of droplets and associated director fields within a class of distortions with cylindrical symmetry, where the total free energy $\mathcal{F}$ in Eq. (38) does *not*

attain a minimum whenever $K_{24} > K_{22}$. We find it convenient to split our discussion into two cases: one where the domain $\mathscr{B}$ can be unbounded and the other where the domain $\mathscr{B}$ is constrained to be bounded.

A. Unconfined drops

Functional $\mathcal{F}_3[\beta]$ in Eq. (34c) is nothing but the dimensionless form taken by the Oseen-Frank elastic free energy in a cylinder subject to degenerate planar boundary conditions [12,29]. Whenever $k_{24} > 1$, the minimizer of $\mathcal{F}_3$ is the escaped twist (ET) field represented by the function

$$\beta_{\rm ET}(\rho) := \arctan\left(\frac{2\sqrt{k_{24}(k_{24}-1)}\rho}{\sqrt{k_3}[k_{24}-(k_{24}-1)\rho^2]}\right), \tag{39}$$

This field together with its chiral variant, represented by the function $\widehat{\beta}_{\rm ET}(\rho) := \pi - \beta_{\rm ET}(\rho)$, describe the director twist within a CLC tactoid (see Fig. 3). They give $\mathcal{F}_3$ one and the same value [12],

$$\mathcal{F}_3[\beta_{\rm ET}] = \mathcal{F}_3[\widehat{\beta}_{\rm ET}] = \begin{cases} 1 - k_{24} + \frac{1}{2}\frac{k_3}{\sqrt{1-k_3}}\,\operatorname{arctanh}\left(\frac{2\sqrt{1-k_3}(k_{24}-1)}{k_3+2(k_{24}-1)}\right), & k_3 \leqq 1, \\ 1 - k_{24} + \frac{1}{2}\frac{k_3}{\sqrt{k_3-1}}\,\arctan\left(\frac{2\sqrt{k_3-1}(k_{24}-1)}{k_3+2(k_{24}-1)}\right), & k_3 \geqq 1. \end{cases} \tag{40}$$

It should be noted that $\mathcal{F}_3[\beta_{\rm ET}] < 0$ and, by Eq. (32), its contribution to the total free energy $\mathcal{F}$ of the drop in Eq. (38) scales like the dominant power in μ as $\mu \to \infty$. This suggests a path capable of driving $\mathcal{F}$ to $-\infty$ along a sequence of needle-shaped twisted tactoids, whose polar span grows indefinitely, while the drop's volume is preserved. For this argument to be conclusive, we need to prove that the contributions to $\mathcal{F}$ other than $\mu\mathcal{F}_3$, which are all positive, are unable to counterbalance the divergence of this latter.

To this end, we take U to be a smooth, positive function in the interval $[-1, 1]$, which obeys Eqs. (30) and (31). Since U is independent of μ, Eq. (31) is asymptotically satisfied for $\mu \to \infty$, provided that U' is bounded and the integrals in Eq. (32) converge. We can now estimate $\mathcal{F}[U, \beta; \mu]$ for any given U in the above admissible class and $\beta = \beta_{\rm ET}$ as $\mu \to \infty$. The leading orders in μ are given by

$$\mathcal{F}[U, \beta_{\rm ET}; \mu, \upsilon] = \mu\mathcal{F}_3[\beta_{\rm ET}] + \upsilon\sqrt{\mu}\int_{-1}^{1} U(\xi)d\xi + \mathcal{O}\left(\frac{\upsilon}{\sqrt{\mu}}\right) \leqq \mu\mathcal{F}_3[\beta_{\rm ET}] + \sqrt{\frac{8}{3}}\upsilon\sqrt{\mu} + \mathcal{O}\left(\frac{\upsilon}{\sqrt{\mu}}\right), \tag{41}$$

where the inequality follows from Hölder's inequality and Eq. (28).[6] Thus, for any admissible function $U = U(\xi)$, in the limit as $\mu \to \infty$ the total free energy of a CLC droplet is shown to be unbounded below whenever $k_{24} > 1$.

Restoring physical units with the aid of Eqs. (38), (33), and (25), to leading orders we can rewrite Eq. (41) as

$$\mathscr{F}[\boldsymbol{n}] \leqq 2\pi\left(K_{22}R_0\mathcal{F}_3[\beta_{\rm ET}] + \sqrt{\frac{8}{3}}\gamma R_{\rm e}^{3/2}R_0^{1/2}\right), \tag{42}$$

which diverges to negative infinity as the span $2R_0$ of the tactoid increases indefinitely.

Clearly, this disconcerting result revolves about $\mathcal{F}_3[\beta_{\rm ET}]$ being negative; one could wonder whether adding a constant to the elastic free-energy density $W_{\rm OF}$ would render $\mathcal{F}_3[\beta_{\rm ET}]$ positive. It is shown in Appendix B that such a simplistic remedy is indeed illusory.

In our development, $\beta_{\rm ET}$ in Eq. (39) plays the role of a test function capable of representing the twisted nematic texture inside a tactoid. We have chosen it as the minimizer of the functional $\mathcal{F}_3$ in Eq. (34c), but any test function that makes $\mathcal{F}_3$ negative for all $k_{24} > 1$ would serve precisely the same purpose. In Appendix C, we show an alternative choice, which has the advantage of giving $\mathcal{F}_3$ a form simpler than Eq. (40).

Here, we have proved that for $k_{24} > 1$ the Oseen-Frank elastic free energy is responsible for the divergence to $-\infty$ of the total free energy of a CLC droplet surrounded by an isotropic fluid enforcing degenerate planar anchoring on the droplet's free boundary. Our proof is based on the construction of a family of filamentous twisted tactoids with a shape chosen arbitrarily within a wide admissible class (see Fig. 4). For definiteness, in Appendix D, we illustrate the details of this construction for a specific drop's profile.

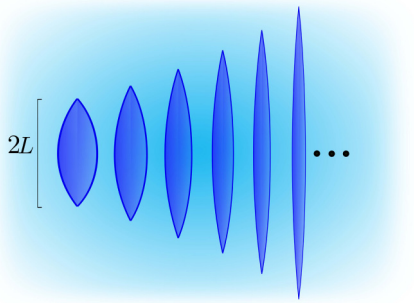

FIG. 4. Sequence of tactoidal drops with fixed volume V_0 and increasing values of μ, the distance between poles scaled to the diameter of the sphere with equal volume. For $k_{24} > 1$, the total free energy diverges to $-\infty$.

B. Confined drops

An objection could be moved against the disruptive argument presented above: in real life, CLC drops cannot be surrounded by an arbitrarily large amount of fluid, so the minimizing sequence shown in Fig. 4 would come to a halt as soon as the drop stretches through the largest available

[6] The classical form of Hölder's inequality estimates the integral of $|gf|$, where f and g are functions defined in a real interval (see, for example, Ref. [30, p. 213]); here it has been applied with $f \equiv 1$ and $g = U$.

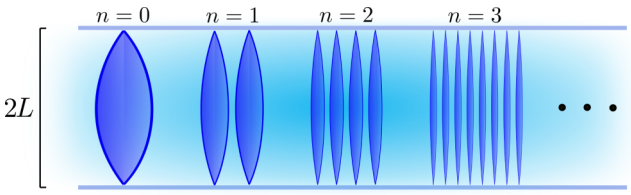

FIG. 5. Splitting procedure described in the text: each droplet splits in halves at every step, thus preserving the total volume. All drops have one and the same polar span $2L$.

length, and no paradox would stand, as the total free energy is finite. Such a pervasive behavior of CLC drops would be too striking to go unnoticed, but, to the best of our knowledge, it has never been observed. There are, however, also strong theoretical reasons to rebut this objection. They are given here.

We study the same problem as in Sec. IV A, but confining drops between two parallel plates, $2L$ apart, and assuming that $2L$ is the maximum polar extension that they have all reached. We start with a single parent drop of given volume V_0 with twisted director field represented by $\beta = \beta_{\rm ET}$ and boundary profile described by a given function $U(\xi)$ (see Fig. 5). The value of μ corresponding to this shape is

$$\mu_0 := \frac{L}{R_{\rm e}}, \tag{43}$$

for which Eq. (38) delivers a finite (dimensionless) total free energy F_0.

We argue that splitting recursively the parent drop in halves, preserving the total volume, will again drive the total free energy to negative infinity. We proceed in steps indexed by the integer $n \in \mathbb{N}$. For $n = 1$, the drop is split in two equal parts; for $n = 2$, each half is again split in two; etcetera, as shown in Fig. 5. The volume of each droplet at step n is $V_n = V_0/2^n$. All droplets have the same polar span $2L$, but since they have different volumes (and so different equivalent radii), the parameter μ defined by Eq. (25) here depends on n too. The equivalent radius R_n of droplets at step n is

$$R_n = 2^{-n/3} R_{\rm e}, \tag{44}$$

so that

$$\mu_n := \frac{L}{R_n} = 2^{n/3}\mu_0 \tag{45}$$

and $\mu_n R_n = \mu_0 R_{\rm e}$ for all n. Not only μ, but also υ, the reduced volume defined by Eq. (33), depends on n:

$$\upsilon_n = \frac{\gamma R_n}{K_{22}} = 2^{-n/3}\upsilon_0, \tag{46}$$

where υ_0 is the reduced volume of the parent drop.

It should be noted that the splitting strategy adopted here affects the droplet's shape, while leaving the function U unchanged. Keeping in mind that the equivalent radius at step n is R_n, we rewrite U as expressed by Eq. (29) in terms of dimensional $R(z)$,

$$U\left(\frac{z}{\mu_n R_n}\right) = \frac{\sqrt{\mu_n}}{R_n} R(z), \tag{47}$$

from which, with the aid of Eqs. (43), (44), and (45), it follows that

$$R(z) = 2^{-n/2} R_{\rm e} \sqrt{\frac{R_{\rm e}}{L}}\, U\left(\frac{z}{L}\right) \quad \text{for} \quad -L \leqq z \leqq L. \tag{48}$$

Similarly, for the total free energy F_n at step n (scaled to $2\pi K_{22} R_{\rm e}$), we readily obtain the estimate

$$\mathsf{F}_n = \frac{R_n}{R_{\rm e}} 2^n \mathcal{F}[U, \beta_{\rm ET}; \mu_n, \upsilon_n] \leqq 2^n \mu_0 \mathcal{F}_3[\beta_{\rm ET}] + \sqrt{\frac{8}{3}} 2^{n/2} \upsilon_0 \sqrt{\mu_0} + \mathcal{O}(2^{-n/2}), \quad n \to \infty. \tag{49}$$

Since $\mathcal{F}_3[\beta_{\rm ET}] < 0$, Eq. (49) implies the divergence of F_n to negative infinity as the splitting proceeds indefinitely.

This confirms that the total free energy of a CLC drop is unbounded below also in the confined case. Being, however, an asymptotic argument, it still leaves room for an objection, more of a physical than mathematical nature. For the above splitting strategy to be interpreted as a shape instability for the parent drop, we should prove that

$$\mathsf{F}_1 < \mathsf{F}_0. \tag{50}$$

It does not suffice to know that $\mathsf{F}_n \to -\infty$. Indeed, it is not difficult to show that for (50) to be valid μ_0 must be sufficiently large. However, as proved in Appendix E, if we split the parent drop in appropriate unequal components, then we can always guarantee the validity of Eq. (50), thus proving that the violation of Ericksen's inequality $K_{22} \geqq K_{24}$ makes a CLC drop unstable against domain splitting.

In the following section, we shall use a similar argument to show that a spherical drop subject to homeotropic anchoring on its boundary would disintegrate if Ericksen's inequality $K_{11} \geqq K_{24}$ is violated.

V. VIOLATING $K_{11} \geqq K_{24}$

Here we assume that $K_{11} < K_{24}$ and consider a spherical droplet $\mathscr{B}_0$ of volume V_0 enforcing *homeotropic anchoring* for the director $\boldsymbol{n}$ on its boundary,

$$\boldsymbol{n}|_{\partial\mathscr{B}_0} \cdot \boldsymbol{\nu} = 1, \tag{51}$$

where $\boldsymbol{\nu}$ is the outer unit normal to $\partial\mathscr{B}_0$. The *radial hedgehog* $\boldsymbol{n}_{\rm H} = \boldsymbol{e}_r$, that is, the director field everywhere directed like the unit vector field $\boldsymbol{e}_r$ emanating from the center of $\mathscr{B}_0$, is a *universal* solution [31]. It satisfies the equilibrium equations associated with any frame-indifferent free-energy density $W(\boldsymbol{n}, \nabla\boldsymbol{n})$.[7] Moreover, $\boldsymbol{n}_{\rm H}$ clearly obeys Eq. (51). With the aid of Eqs. (1) and (10), the total free-energy functional $\mathscr{F}$ in Eq. (11) is readily computed for $\boldsymbol{n}_{\rm H}$; its scaled value is

$$\mathcal{F}^* := \frac{\mathscr{F}[\boldsymbol{n}_{\rm H}]}{4\pi K_{11} R_{\rm e}} = 1 - k_{24}^* + \upsilon^*(1+\omega), \tag{52}$$

[7] Since the Oseen-Frank energy density $W_{\rm OF}$ in Eq. (2) is frame-indifferent, $\boldsymbol{n}_{\rm H}$ is an equilibrium solution for $\mathscr{F}$, for any choice of the elastic constants.

where, in analogy with Eqs. (35) and (33), we have set

$$k_{24}^* := \frac{K_{24}}{K_{11}} > 1 \quad \text{and} \quad \upsilon^* := \frac{\gamma R_e}{K_{11}}. \tag{53}$$

We now proceed as in Sec. IV B, splitting the drop into 2^n equal spherical components, each of radius R_n as in Eq. (44). The formula for the total free energy F_n^* (scaled to $4\pi K_{11} R_e$) that mimics Eq. (49) is here

$$\begin{aligned}\mathsf{F}_n^* &= 2^{2n/3}[(1-k_{24}^*) + 2^{-n/3}\upsilon^*(1+\omega)] \\ &= 2^{2n/3}(1-k_{24}^*) + \mathcal{O}(2^{n/3}) \to -\infty, \quad n \to \infty,\end{aligned} \tag{54}$$

which proves the asymptotic instability of the parent spherical drop when the Ericksen inequality $K_{11} \geqq K_{24}$ is violated.

As already remarked in Sec. IV B, this reasoning does not guarantee that the parent spherical drop splits spontaneously in halves. For this to be the case, it must be $\mathsf{F}_1^* < \mathsf{F}_0^*$, which requires that

$$\upsilon^* < \frac{(k_{24}^*-1)}{(1+\omega)} \frac{(2^{2/3}-1)}{(2^{1/3}-1)}, \tag{55}$$

thus setting an effective upper bound on the drop's initial volume.

A drop is however unstable also when Eq. (55) is not satisfied. To see this, for given $0 < \lambda < \frac{1}{2}$, we split the parent drop into two *unequal* spherical components, with volumes V_1 and V_2 adding up to V_0,

$$V_1 = \lambda V_0, \quad V_2 = (1-\lambda)V_0 \tag{56}$$

and corresponding radii

$$R_1 = \lambda^{1/3} R_e, \quad R_2 = (1-\lambda)^{1/3} R_e. \tag{57}$$

The total free energy F_λ^* (again scaled to $4\pi K_{11} R_e$) is now given by

$$\begin{aligned}\mathsf{F}_\lambda^* &= \lambda^{1/3}[(1-k_{24}^*) + \lambda^{1/3}\upsilon^*(1+\omega)] \\ &\quad + (1-\lambda)^{1/3}[(1-k_{24}^*) + (1-\lambda)^{1/3}\upsilon^*(1+\omega)],\end{aligned} \tag{58}$$

and the inequality $\mathsf{F}_\lambda^* < \mathsf{F}_0^*$ is satisfied for

$$\begin{aligned}\upsilon^* &< \frac{(k_{24}^*-1)}{(1+\omega)} \frac{[\lambda^{1/3} + (1-\lambda)^{1/3} - 1]}{[\lambda^{2/3} + (1-\lambda)^{2/3} - 1]} = \mathcal{O}(\lambda^{-1/3}) \\ &\to +\infty, \quad \lambda \to 0.\end{aligned} \tag{59}$$

Thus, for every given volume of the drop there is a splitting fraction $\lambda > 0$ corresponding to a net decrease in the total free energy.

VI. CONCLUSIONS

This paper shows the paradoxical consequences stemming from adopting the classical Oseen-Frank elastic theory to describe CLCs when either of the following Ericksen inequalities is violated,

$$K_{22} \geqq K_{24}, \tag{60a}$$

$$K_{11} \geqq K_{24}. \tag{60b}$$

Violation of the former is at the heart of the commonly accepted understanding of CLCs, as it substantiates the experimentally observed ground state of these materials, which in capillary cylinders with degenerate planar boundary conditions take one of two symmetric twisted director configurations.

As shown in Ref. [12], violation of Eq. (60a) in the presence of degenerate planar anchoring is *not* prejudicial to the stability of the twisted ground state (see also Ref. [13]); this has perhaps nurtured the hope that Eq. (60a) may be renounced in the Oseen-Frank theory of CLCs. Our paper proves that this is not the case, as such a relaxed theory would entail shape instability of tactoids, an instability which contradicts a full body of solid experimental evidence, and which we deem paradoxical.

When Eq. (60b) is violated, a similar shape instability is predicted, this time for spherical droplets with homeotropic anchoring. We know about only one material for which both inequalities in Eq. (60) are allegedly violated. This is SSY, for which the following values of the elastic constants were measured in Ref. [32], $K_{11} = 4.3$pN, $K_{22} = 0.7$pN, and $K_{33} = 6.1$pN, and it was found in Ref. [7] that $K_{24} = 15.8$pN. These experimental values were obtained by assuming valid the Oseen-Frank theory.

We cannot justify within the Oseen-Frank theory both the observed ground state of CLCs and their ability to form stable twisted tactoids. We see two ways to avoid this contradiction: either (i) the common interpretation of the capillary experiments that established the CLC ground state is incorrect, or (ii) the Oseen-Frank theory is inapt to describe the elasticity of these materials. Boundary conditions are instrumental to alternative (i): one might question whether a mild azimuthal anchoring is at work, which could alter the determination of K_{24} so that the Ericksen inequalities are not violated. Here we trust the detailed experimental analysis of the capillaries' inner boundary performed in Ref. [7] with the aid of both atomic force microscopy (AFM) and scanning electron microscopy (SEM)[8]; it was concluded that any azimuthal anchoring, if at all present, must be negligible compared with the saddle-splay energy, thus fully supporting the hypothesis of a pure degenerate planar anchoring. In want of further experimental data, we are inclined towards alternative (ii): we reckon worth pursuing a novel elastic theory for CLCs. Some timid proposals have already been advanced. For example, in Ref. [13] the role of added disclinations is advocated (provided that their energy cost can be made sufficiently low), whereas in Ref. [33] a quartic twist term is added to the Oseen-Frank free-energy density, which has the potential to restore shape stability when Eq. (60a) is violated [but Eq. (60b) is not]. We are presently favoring this line of thought, although we are aware that it may suffer from the many difficulties encountered by other higher-order theories.

APPENDIX A: USEFUL COMPUTATIONS

This technical Appendix contains ancillary results used in Sec. III. For the particular class of distortions

[8]See also the supplementary information of Ref. [7] and the AFM measurements of Ref. [6].

described by Eq. (17) with α a smooth function of z, we compute

$$\begin{aligned}\nabla \boldsymbol{n} = \frac{1}{R}\Big\{ &\cos\alpha\cos\beta\beta'\boldsymbol{e}_r\otimes\boldsymbol{e}_r - \frac{1}{\rho}\sin\alpha\sin\beta\boldsymbol{e}_r\otimes\boldsymbol{e}_\theta - (\sin\alpha\sin\beta\alpha' R + \rho R'\cos\alpha\cos\beta\beta')\boldsymbol{e}_r\otimes\boldsymbol{e}_z\\ &+ \sin\alpha\cos\beta\beta'\boldsymbol{e}_\theta\otimes\boldsymbol{e}_r + \frac{1}{\rho}\cos\alpha\sin\beta\boldsymbol{e}_\theta\otimes\boldsymbol{e}_\theta + (\cos\alpha\sin\beta\alpha' R - \rho R'\sin\alpha\cos\beta\beta')\boldsymbol{e}_\theta\otimes\boldsymbol{e}_z\\ &- \sin\beta\beta'\boldsymbol{e}_z\otimes\boldsymbol{e}_r + \rho R'\sin\beta\beta'\boldsymbol{e}_z\otimes\boldsymbol{e}_z\Big\},\end{aligned} \tag{A1}$$

where, as in the main text, a prime denotes differentiation.

The following identities justify the expression for the reduced functionals (32a) and (32b); they are obtained making use of Eq. (19),

$$\int_{-\mu}^{\mu}\cos^2\alpha dz = \frac{1}{\tan^2\beta(1)}\int_{-\mu}^{\mu}R'^2dz = \frac{1}{\mu^2\tan^2\beta(1)}\int_{-1}^{1}U'^2d\xi, \tag{A2a}$$

$$\int_{-\mu}^{\mu}\sin\alpha\alpha' R dz = -\frac{1}{\tan\beta(1)}\int_{-\mu}^{\mu}R'' R dz = \frac{1}{\tan\beta(1)}\int_{-\mu}^{\mu}R'^2dz = \frac{1}{\mu^2\tan\beta(1)}\int_{-1}^{1}U'^2d\xi, \tag{A2b}$$

$$\int_{-\mu}^{\mu}\alpha'^2R^2dz = \int_{-\mu}^{\mu}\frac{R''^2R^2}{\tan\beta(1)^2 - R'^2}dz = \frac{1}{\mu^2}\int_{-1}^{1}\frac{U''^2U^2}{\mu^3\tan\beta(1)^2 - U'^2}d\xi. \tag{A2c}$$

Here ξ is the variable defined in Eq. (27) and an integration by parts has been performed in Eq. (A2b) with the aid of Eq. (30).

APPENDIX B: USELESS CONSTANT

When $k_{24} > 1$, the ET configuration (39) realizes the minimum of $\mathcal{F}_3[\beta]$, the dimensionless form of the Oseen-Frank elastic free energy in a cylinder subject to degenerate boundary conditions, and possess less elastic free energy than the uniform alignment $\boldsymbol{n} = \boldsymbol{e}_z$, described by $\beta \equiv 0$, for which $\mathcal{F}_3$ vanishes.

We have seen that the divergence to negative infinity of the functional in Eq. (38) in the sequences of droplets considered in Sec. V stems from being $\mathcal{F}_3[\beta_{\rm ET}] < 0$. One could wonder whether the Oseen-Frank energy density $W_{\rm OF}$ might be altered by an additive constant c chosen to make positive the minimum energy of the ET configuration in a cylinder. This question is easily answered for the positive, but it turns out that c depends on the cylinder's radius R,

$$c = -\frac{2K_{22}}{R^2}\mathcal{F}_3[\beta_{\rm ET}], \tag{B1}$$

and, failing to be intrinsic, it is of no use.

APPENDIX C: ALTERNATIVE TEST FUNCTION

Functional $\mathcal{F}_3[\beta]$ in Eq. (34c) could be negative for every $k_{24} > 1$ also when the function β is different from $\beta_{\rm ET}$ in Eq. (39). Let the function β_ω be defined as

$$\beta_\omega(\rho) := \arctan(\omega\rho). \tag{C1}$$

Here ω is a parameter to be chosen to minimize $\mathcal{F}_3[\beta_\omega]$. A simple calculation delivers

$$\mathcal{F}_3[\beta_\omega] = \frac{k_3}{4}\ln\left(1+\omega^2\right) + \frac{\omega^2}{4(1+\omega^2)}[k_3 + 4(k_{24}-1)], \tag{C2}$$

which is minimized for

$$\omega = \bar\omega := \begin{cases}\frac{2\sqrt{k_{24}-1}}{\sqrt{k_3}}, & k_{24} \geqq 1,\\ 0, & k_{24} \leqq 1.\end{cases} \tag{C3}$$

Correspondingly, for $k_{24} > 1$,

$$\mathcal{F}_3[\beta_{\bar\omega}] = \frac{k_3}{2}\operatorname{arctanh}\left[\frac{2(k_{24}-1)}{k_3 + 2(k_{24}-1)}\right] + 1 - k_{24} < 0. \tag{C4}$$

Clearly, as is not difficult to check directly, $\mathcal{F}_3[\beta_{\rm ET}] < \mathcal{F}_3[\beta_{\bar\omega}]$.

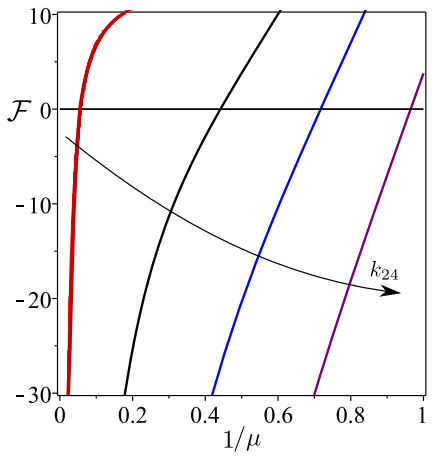

FIG. 6. Graphs of $\mathcal{F}$ in Eq. (38) against $1/\mu$ for U as in Eq. (D1) and $\beta = \beta_{\rm ET}$ as in Eq. (39) for $k_1 = k_3 = 10$, $\upsilon = 10$ and a sequence of values of $k_{24} > 1$, precisely, $k_{24} = 1.2$, 4., 7.5, 12 (arranged in increasing order, as indicated by the arrow). Whenever $k_{24} > 1$, $\mathcal{F}$ is unbounded below and diverges to $-\infty$ as μ tends to ∞.

APPENDIX D: SINUSOIDAL PROFILE

We present here an illustrative example, in which the drop's profile is described by the following sinusoidal function

$$U = \frac{2}{\sqrt{3}} \cos\left(\frac{\pi\xi}{2}\right), \tag{D1}$$

which vanishes at the poles, where $\xi = \pm 1$, and satisfies Eq. (28). For U as in Eq. (D1), Eq. (31) is satisfied whenever

$$\mu \geqq \frac{1}{3^{1/3}2^{1/3}} \left[\frac{\sqrt{k_3}}{\sqrt{k_{24}(k_{24}-1)}}\right]^{2/3}. \tag{D2}$$

The functional $\mathcal{F}$ in Eq. (38) has been computed numerically for U as in Eq. (D1), $\beta = \beta_{\rm ET}$, and μ satisfying Eq. (D2). The outcome is illustrated by the graphs shown in Fig. 6 for $k_1 = k_3 = 10$, $\upsilon = 10$, and different values of $k_{24} > 1$. For every $k_{24} > 1$, in the limit as μ tends to ∞, $\mathcal{F}$ does not attain a minimum and diverges to $-\infty$, as expected.

APPENDIX E: DESTABILIZING SPLITTING

In this Appendix, we reason as in Sec. V to show that when $k_{24} > 1$ a confined droplet can be split into two *unequal* components in such a way that the total free energy is decreased.

Let $0 < \lambda < \frac{1}{2}$ be given and let the volumes of the split droplets V_1 and V_2 be defined as in Eq. (56), for which R_1 and R_2 in Eq. (57) play the role of equivalent radii. Correspondingly, there are two parameters defined for each droplet as in Eq. (43),

$$\mu_1 = \lambda^{-1/3}\mu_0, \quad \mu_2 = (1-\lambda)^{-1/3}\mu_0, \tag{E1}$$

and two dimensionless volumes,

$$\upsilon_1 = \lambda^{1/3}\upsilon, \quad \upsilon_2 = (1-\lambda)^{1/3}\upsilon. \tag{E2}$$

In analogy with Eq. (49), the total free energy F_λ of the pair of split droplets (scaled to $2\pi K_{22}R_{\rm e}$) is given by

$$\mathsf{F}_\lambda = \lambda^{1/3}\mathcal{F}[U, \beta_{\rm ET}; \mu_1, \upsilon_1] + (1-\lambda^{1/3})\mathcal{F}[U, \beta_{\rm ET}; \mu_2, \upsilon_2], \tag{E3}$$

where $\mathcal{F}$ is delivered by Eq. (38). To ease our proof, with the aid of Eqs. (32) and (34), we now rewrite $\mathcal{F}$ in Eq. (38) as

$$\mathcal{F}[U, \beta; \mu, \upsilon] = \tfrac{1}{\mu^2}\mathsf{G}_1[U]\mathcal{F}_1[\beta] + \tfrac{1}{\mu^2}\mathsf{G}_2[U;\mu]\mathcal{F}_2[\beta] + \mu\mathcal{F}_3[\beta] + \upsilon\sqrt{\mu}\mathsf{G}_{\rm s}[U;\mu], \tag{E4}$$

where we have set

$$\mathsf{G}_1[U] := \int_{-1}^{1} U'(\xi)^2 d\xi, \quad \mathsf{G}_2[U;\mu] := \int_{-1}^{1} \frac{U(\xi)^2 U''(\xi)^2}{\mu^3 \tan^2\beta(1) - U'(\xi)^2} d\xi, \quad \mathsf{G}_{\rm s}[U;\mu] := \int_{-1}^{1} U(\xi)\sqrt{1 + \frac{U'(\xi)^2}{\mu}}\, d\xi. \tag{E5}$$

Since both G_2 and $\mathsf{G}_{\rm s}$ are monotonically decreasing in μ and, by Eq. (E1), $\mu_i > \mu_0$, for $i = 1, 2$, we readily see from Eq. (E4) that

$$\begin{aligned}\mathsf{F}_\lambda &< \tfrac{1}{\mu_0^2}\mathsf{G}_1[U]\mathcal{F}_1[\beta_{\rm ET}] + \tfrac{1}{\mu_0^2}\mathsf{G}_2[U;\mu_0]\mathcal{F}[\beta_{\rm ET}] + 2\mu_0\mathcal{F}_3[\beta_{\rm ET}] + \upsilon\sqrt{\mu_0}[\lambda^{1/2} + (1-\lambda)^{1/2}]\mathsf{G}_{\rm s}[U;\mu_0] \\ &= \mathsf{F}_0 + \mu_0\mathcal{F}_3[\beta_{\rm ET}] + \upsilon\sqrt{\mu_0}[\lambda^{1/2} + (1-\lambda)^{1/2} - 1]\mathsf{G}_{\rm s}[U;\mu_0],\end{aligned} \tag{E6}$$

where F_0 is the total free energy of the parent drop. The inequality $\mathsf{F}_\lambda < \mathsf{F}_0$ is then valid for

$$\upsilon < -\frac{\sqrt{\mu_0}}{[\lambda^{1/2} + (1-\lambda)^{1/2} - 1]} \frac{\mathcal{F}_3[\beta_{\rm ET}]}{\mathsf{G}_{\rm s}[U;\mu_0]} = \mathcal{O}(\lambda^{-1/2}) \to +\infty, \quad \lambda \to 0. \tag{E7}$$

The divergence of this upper bound for υ as λ tends to 0 guarantees that there is always a $\bar{\lambda} \in (0, \frac{1}{2}]$ such that for every $\lambda \in (0, \bar{\lambda})$ the inequality (E7) is satisfied for a given υ, and so the parent drop is unstable.

[1] J. Lydon, Chromonic liquid crystal phases, Curr. Opin. Colloid Interface Sci. **3**, 458 (1998).

[2] J. Lydon, Chromonics, in *Handbook of Liquid Crystals: Low Molecular Weight Liquid Crystals II* (John Wiley & Sons, Weinheim, 1998), Chap. XVIII, pp. 981–1007.

[3] J. Lydon, Chromonic review, J. Mater. Chem. **20**, 10071 (2010).

[4] J. Lydon, Chromonic liquid crystalline phases, Liq. Cryst. **38**, 1663 (2011).

[5] I. Dierking and A. Martins Figueiredo Neto, Novel trends in lyotropic liquid crystals, Crystals **10**, 604 (2020).

[6] K. Nayani, R. Chang, J. Fu, P. W. Ellis, A. Fernandez-Nieves, J. O. Park, and M. Srinivasarao, Spontaneous emergence of chirality in achiral lyotropic chromonic liquid crystals confined to cylinders, Nat. Commun. **6**, 8067 (2015).

[7] Z. S. Davidson, L. Kang, J. Jeong, T. Still, P. J. Collings, T. C. Lubensky, and A. G. Yodh, Chiral structures and defects of lyotropic chromonic liquid crystals induced by saddle-splay elasticity, Phys. Rev. E **91**, 050501(R) (2015); see also Erratum [34] and Supplemental Material at https://journals.aps.org/pre/supplemental/10.1103/PhysRevE.91.050501/Supplementary_Info_Planar_Davidson_et_al.pdf.

[8] J. Fu, K. Nayani, J. Park, and M. Srinivasarao, Spontaneous emergence of twist and formation of monodomain in lyotropic chromonic liquid crystals confined to capillaries, NPG Asia Mater. **9**, e393 (2017).

[9] A. Javadi, J. Eun, and J. Jeong, Cylindrical nematic liquid crystal shell: Effect of saddle-splay elasticity, Soft Matter **14**, 9005 (2018).
[10] E. G. Virga, Uniform distortions and generalized elasticity of liquid crystals, Phys. Rev. E **100**, 052701 (2019).
[11] J. L. Ericksen, Inequalities in liquid crystal theory, Phys. Fluids **9**, 1205 (1966).
[12] S. Paparini and E. G. Virga, Stability against the odds: The case of chromonic liquid crystals, J. Nonlin. Sci. **32**, 74 (2022).
[13] C. Long and J. V. Selinger, Violation of Ericksen inequalities in lyotropic chromonic liquid crystals J. Elast. (2022).
[14] L. Tortora, H.-S. Park, S.-W. Kang, V. Savaryn, S.-H. Hong, K. Kaznatcheev, D. Finotello, S. Sprunt, S. Kumar, and O. D. Lavrentovich, Self-assembly, condensation, and order in aqueous lyotropic chromonic liquid crystals crowded with additives, Soft Matter **6**, 4157 (2010).
[15] L. Tortora and O. D. Lavrentovich, Chiral symmetry breaking by spatial confinement in tactoidal droplets of lyotropic chromonic liquid crystals, Proc. Natl. Acad. Sci. USA **108**, 5163 (2011).
[16] C. Peng and O. D. Lavrentovich, Chirality amplification and detection by tactoids of lyotropic chromonic liquid crystals, Soft Matter **11**, 7221 (2015).
[17] K. Nayani, J. Fu, R. Chang, J. O. Park, and M. Srinivasarao, Using chiral tactoids as optical probes to study the aggregation behavior of chromonics, Proc. Natl. Acad. Sci. USA **114**, 3826 (2017).
[18] S. Shadpour, J. P. Vanegas, A. Nemati, and T. Hegmann, Amplification of chirality by adenosine monophosphate-capped luminescent gold nanoclusters in nematic lyotropic chromonic liquid crystal tactoids, ACS Omega **4**, 1662 (2019).
[19] C. W. Oseen, The theory of liquid crystals, Trans. Faraday Soc. **29**, 883 (1933).
[20] F. C. Frank, On the theory of liquid crystals, Discuss. Faraday Soc. **25**, 19 (1958).
[21] H. Zocher, The effect of a magnetic field on the nematic state, Trans. Faraday Soc. **29**, 945 (1933).
[22] E. G. Virga, *Variational Theories for Liquid Crystals*, Applied Mathematics and Mathematical Computation Vol. 8 (Chapman & Hall, London, UK, 1994).
[23] J. V. Selinger, Interpretation of saddle-splay and the Oseen-Frank free energy in liquid crystals, Liq. Cryst. Rev. **6**, 129 (2018).
[24] T. Machon and G. P. Alexander, Umbilic Lines in Orientational Order, Phys. Rev. X **6**, 011033 (2016).
[25] J. V. Selinger, Director deformations, geometric frustration, and modulated phases in liquid crystals, Annu. Rev. Condens. Matter Phys. **13**, 49 (2022).
[26] A. Pedrini and E. G. Virga, Liquid crystal distortions revealed by an octupolar tensor, Phys. Rev. E **101**, 012703 (2020).
[27] A. Rapini and M. Papoular, Distorsion d'une lamelle mématique sous champ magnétique conditions d'ancrage aux parois, J. Phys. Colloq. **30**, C4-54 (1969).
[28] S. Paparini and E. G. Virga, Nematic tactoid population, Phys. Rev. E **103**, 022707 (2021).
[29] S. Burylov, Equilibrium configuration of a nematic liquid crystal confined to a cylindrical cavity, J. Exp. Theor. Phys. **85**, 873 (1997).
[30] H. L. Royden, *Real Analysis*, 2nd ed. (MacMillan, New York, 1968).
[31] J. L. Ericksen, General solutions in the hydrostatic theory of liquid crystals, Trans. Soc. Rheol. **11**, 5 (1967).
[32] S. Zhou, Y. A. Nastishin, M. M. Omelchenko, L. Tortora, V. G. Nazarenko, O. P. Boiko, T. Ostapenko, T. Hu, C. C. Almasan, S. N. Sprunt, J. T. Gleeson, and O. D. Lavrentovich, Elasticity of Lyotropic Chromonic Liquid Crystals Probed by Director Reorientation in a Magnetic Field, Phys. Rev. Lett. **109**, 037801 (2012).
[33] S. Paparini, Mathematical Models for Chromonic Liquid Crystals, Ph.D. thesis, Joint Ph.D. Program in Mathematics, Pavia-Milano Bicocca-INdAM, Milan (2022).
[34] Z. S. Davidson, L. Kang, J. Jeong, T. Still, P. J. Collings, T. C. Lubensky, and A. G. Yodh, Erratum: Chiral structures and defects of lyotropic chromonic liquid crystals induced by saddle-splay elasticity [Phys. Rev. E 91, 050501(R) (2015)], Phys. Rev. E **92**, 019905(E) (2015).